Review Article

Cone beam computed tomography in oral implants

Jyoti Gupta, Syed Parveez Ali

Department of Oral Medicine and Radiology, KIMSU School of Dental Sciences, Karad, Maharashtra, India

ABSTRACT

Cone beam computed tomography (CBCT) scanners for the oral and maxillofacial region were pioneered in the late 1990s independently by Arai *et al.* in Japan and Mozzo *et al*. CBCT has a lower dose of radiation, minimal metal artifacts, reduced costs, easier accessibility, and easier handling than multislice computed tomography (MSCT); however, the latter is still considered a better choice for the analysis of bone density using a Hounsfield unit (HU) scale. Oral implants require localized area of oral and maxillofacial area for radiation exposure; so, CBCT is an ideal choice. CBCT scans help in the planning of oral implants; they enable measurement of the distance between the alveolar crest and mandibular canal to avoid impingement of inferior alveolar nerve, avoid perforation of the mandibular posterior lingual undercut, and assess the density and quality of bone, and help in planning of the oral implant in the maxilla with special attention to the nasopalatine canal and maxillary sinus. Hence, CBCT reduces the overall exposure to radiation.

Address for correspondence:
Dr. Syed Parveez Ali,
Ummer Khyam Road, Eidgah,
Tilak Nagar, Mysore - 570 021,
Karnataka, India.
E-mail: dr.parveez@gmail.com

Key words: Cone beam computed tomography, Hounsfield units, multislice computed tomography

Introduction

Cone beam computed tomography (CBCT) was introduced to the dental field to replace the cumbersome, expensive, and high-radiation–producing medical CT scans around a decade ago[1] Suomalainen *et al*.[2] found that the CBCT scans were more accurate than CT scans. The American Association of Oral and Maxillofacial Radiology has stated that cross-sectional views are recommended for planning dental implants, and this in combination with the easy accessibility, easy handling, and low-radiation dose of CBCT imaging will lead to the widespread use of CBCT imaging in implantology.[3] Considering the dose of radiation from other image acquisition modalities such as multislice computed tomography (MSCT, e.g., MaxMand CT scan: Effective dose of 2100 according to the 1990 recommendations of the International Commission on Radiological Protection (ICRP))[4] and panoramic radiography (e.g., panoramic OrthoPhos Plus: Effective dose of 6.3 and 13.3 according to ICRP 1990 and 2005, respectively),[5] CBCT has lesser radiation than MSCT and 10 times more radiation than a panoramic X-ray. The dose of radiation should be reported in millisievert (mSv) or microsievert (μSv) to express the effective dose (E). As Ludlow[6] stated, the E of radiation has been recommended by the ICRP[7] as a means of comparing the detriment of different exposures to ionizing radiation to an equivalent detriment produced by a full-body dose of radiation. The E should be calculated using the equation E = PwT_HT, where wT = weighting factor, HT = equivalent dose. The HT should be calculated using the equation HT = PwR_DT, where wR = radiation weighting factor (which is 1 in the case of X-ray radiation), DT = absorbed dose.[7] Benefits of CBCT are three-dimensional (3D) dataset, real-size data, the potential for generating all 2D images (e.g., orthopantomogram, lateral cephalogram, imaging of the temporomandibular joint (TMJ)), potential for vertical scanning in a natural seated position, isotropic voxel size, high-resolution (e.g., bone trabeculae, periodontal ligament (PDL), root formation) imaging, lower dose of radiation than MSCT, less disturbance from metal artifacts, reduced costs compared with MSCT, easier accessibility, in-office imaging, easier handling, small footprint, Digital Imaging and Communications

Access this article online

Quick Response Code:

Website: www.njms.in

DOI: 10.4103/0975-5950.117811

in Medicine (DICOM) compatiblity, user-friendly postprocessing and viewing software, and better saving of energy compared with MSCT.[1] Limitations are low contrast range, limited detector size causing limited field of view and limited scanned volume, limited inner soft tissue information, increased noise from scatter radiation and concomitant loss of contrast resolution, movement of artifacts affecting the whole dataset, truncation artifacts (caused by the fact that projections acquired with the region of interest selection do not contain the entire object), and that they cannot be used for estimation of Hounsfield units (HUs).[1] HUs represent the relative density of body tissues according to a calibrated gray-level scale, based on normalized HU values for air (−1000 HU), water (0 HU), and dense bone (+1000 HU). HUs are standard numbers originating from conventional MSCT imaging.[8] Despite the advantages of CBCT compared with MSCT imaging, the latter is still considered a better choice for the analysis of bone density using an HU scale.[9-11] The fan-shaped X-ray beam associated with less scattering and artifact production may explain the better accuracy of intensity values in an MSCT than in a CBCT scanner which is a cone-shaped X-ray beam, and its higher amount of scattering and artifacts may explain the inaccuracies of their intensity values.[12] In both technologies, the accuracy of intensity values can be affected by the beam-hardening phenomenon, which causes artifacts on the reconstructed images.[13]

Mandibular lingual undercut and inferior alveolar canal

In the posterior mandibular region, a deep lingual undercut is a common finding and can be difficult to manage, especially when a lingual plate perforation is suspected. It is essential to check the angulations and positioning of the drills or implant fixtures via radiographs and clinical detection of a possible perforation in the osteotomy site. For preoperative implants, CTs are preferred because cross-sectional views bring a clearer visualization of the anatomy of the surgical site [Figure 1].[14,15] The major potential risks of encountering a lingual plate perforation are massive hemorrhage of submental and sublingual arteries,[16] airway obstruction,[17] and a perforation above the mylohyoid ridge might injure the lingual nerve.[18] If the extruded implant is left unattended, the infection might spread to the parapharyngeal and retropharyngeal space, leading to more severe complications, such as mediastinitis, mycotic aneurysm formation with possible subsequent rupture of the internal carotid artery, and internal jugular vein thrombosis with septic pulmonary embolism or upper airway obstruction.[19,20] The experimental site has to have sufficient vertical bone height (12 mm from the alveolar crest to the superior border of the inferior alveolar nerve canal (IAN)) to possibly place a 10 mm implant and a minimum gap of

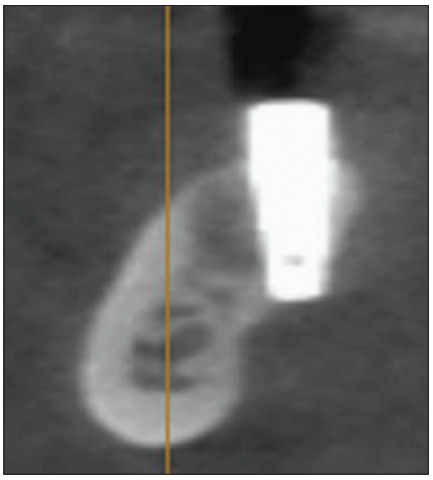

Figure 1: Cone beam computed tomography image demonstrating the possibility of lingual plate perforation by an implant

2 mm between the tip of implant and mandibular canal.[21] The experimental site has to have adequate horizontal bone width (3.5 mm).[22] Mandibular cross-sectional imaging at the edentulous first molar region shows three types of morphologies. The undercut ridge type (type U, 66%) is a ridge with a narrow base that expands bucco-lingually to a wider crest with a prominent point (point P) on the lingual plate, giving rise to a lingual undercut. The parallel ridge type (type P, 20.4%) ridge generally has a more or less parallel ridge form; no lingual undercut is seen. The convergent ridge type (type C, 13.6%) ridge is one where the base of the ridge is wider than its crest; no obvious undercut is seen [Figure 2].[22]

Watanabe *et al*. classified the cross-sectional mandibular morphology based on the outlines of the lingual and buccal plates, round on the buccal side and concave on the lingual side (type A), concave on the buccal side and round on the lingual side (type B), and round shape on both sides (type C). They reported that at the posterior region, type C (round) was the most commonly found (59-61%), followed by type A (lingual concavity) (36-39%).[23] The width of the mandible 5-20 mm from the inferior border of the mandible ranged from 10.5 to 15.8 mm, with no significant differences between genders.[23] Panoramic radiographs have an inherent magnification ranging from 10 to 30%, with the horizontal magnification being more variable and thus less reliable.[24] Marginal loss of bone and loss of bone-to-implant contact (e.g., by marsupuilization) may indeed negatively influence success of the implant.[25] Several criteria have been proposed to analyze oral implants radiologically. Most of these studies suggest an acceptable average of marginal loss of bone (bone loss of 2 mm after the first year) and the absence of a peri-implant radiolucency as a criterion of radiological success.[26]

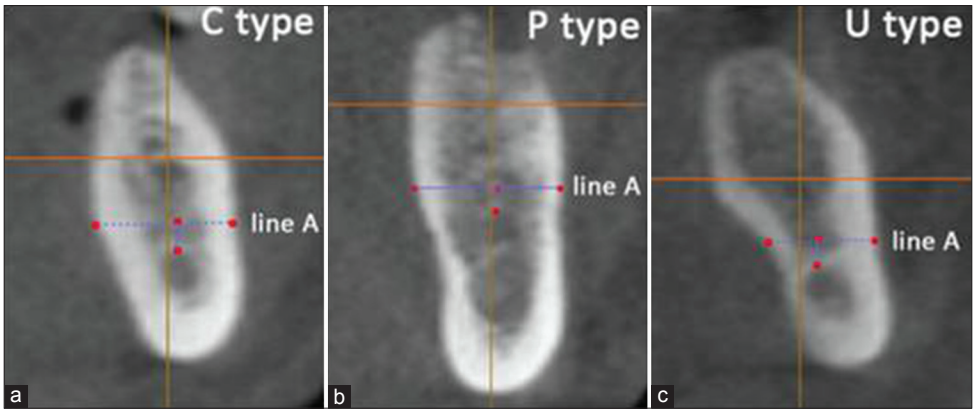

Figure 2: Three types of cross-sectional posterior mandibular morphology: (a) C type, (b) P type, and (c) U type; line A represented a reference line 2 mm coronal to the inferior alveolar nerve canal

Accessory mental foramen

The mandibular canal and mental foramen involve the inferior alveolar artery and inferior alveolar nerve. Because images of the accessory mental foramina and bony canal to the accessory mental foramen overlap in various trabecular bone patterns.[27] It was reported that the presence of the bifid mandibular canal in the mandibular ramus region was observed more frequently with CBCT images, in 65% of patients[28] compared with rotational panoramic radiographs, with a range from 0.08 to 0.95%.[29] The accessory mental nerve communicated with branches of the facial and buccal nerves. So, it was indicated that surgical complications might be attributed to the existence of a mandibular incisive canal with a true neurovascular supply, and potential risks might also be related to the presence of the lingual foramen and anatomic variations, such as an anterior looping of the mental nerve [Figure 3].[30]

Nasopalatine morphology

The nasopalatine canal is usually described as being located in the midline of the palate, posterior to the central maxillary incisors. The funnel-shaped oral opening of the canal in the midline of the anterior palate is known as the incisive foramen, and is usually located immediately below the incisive papilla. The canal divides into two canaliculi on its way to the nasal cavity, and terminates at the nasal floor with an opening (known as the foramina of Stenson) at either side of the septum. The canal contains the nasopalatine (incisive) nerve and the terminal branch of the descending nasopalatine artery, as well as fibrous connective tissue, fat, and even small salivary glands. Contact of the implant with neural tissue may result in failure of osseointegration or lead to sensory dysfunction.[31] The anatomic variants of the canal are differentiated into three groups [Figures 4 and 5].

Alveolar process

Dimensional alterations occur on the alveolar process following tooth extraction.[32,33] After the healing process

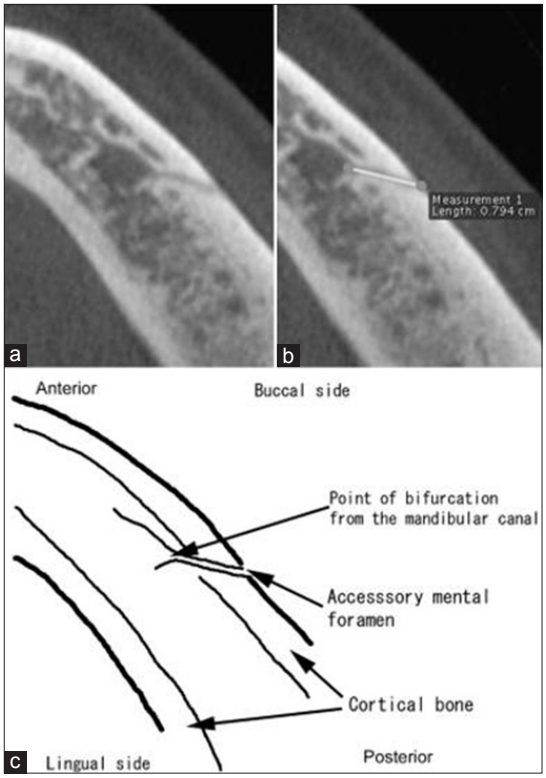

Figure 3: Measurement between the accessory mental foramen and point of bifurcation from the mandibular canal: (a) Two-dimensional cone beam computed tomography image of the accessory mental foramen and point of bifurcation from the mandibular canal; (b) Linear distance between the accessory mental foramen and point of bifurcation from the mandibular canal; (c) Schematic drawing of 2D CBCT image (a)

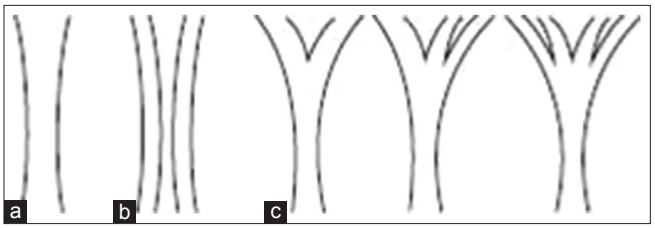

Figure 4: Classification of anatomic variations of the nasopalatine canal:(a) A single canal; (b) Two parallel canals; (c) Variations of the Y type of canal, with one oral/palatal opening (¼ incisive foramen) and two or more nasal openings (¼ foramina of Stenson)

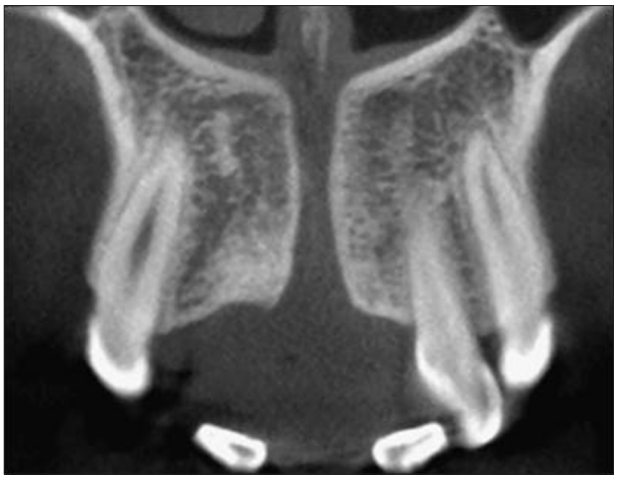

Figure 5a: Type A nasopalatine canal (a single canal)

Figure 5b: Type B nasopalatine canal (two separate canals) as evaluated in a coronal cone beam computed tomography image

Figure 5c: Type C nasopalatine canal (Y configuration of canal) with one oral/palatal opening and two nasal openings

is completed, loss of bone at the facial aspect of the marginal one-third of the socket is more pronounced than in the palatal/lingual aspect. This difference in the healing outcome maybe related to the fact that the buccal bone wall is thinner than its palatal counterpart. Placement of implant in fresh extraction sockets could counteract ridge resorption. The thinner the facial bone wall, the more extensive the loss of facial bone.[34] Following tooth removal/loss, the entire marginal, buccal bone plate be lost, but an additional 2 mm of the original socket dimension may disappear during the process of socket healing and site adaptation.[34]

References

1. De Vos W, Casselman J, Swennen GR. Cone-beam computerized tomography (CBCT) imaging of the oral and maxillofacial region: A systematic review of the literature. Int J Oral Maxillofac Surg 2009;38:609-25.
2. Arai Y, Tammisalo E, Iwai K, Hashimoto K, Shinoda K. Development of a compact computed tomographic apparatus for dental use. Dentomaxillofac Radiol 1999;28:245-8.
3. Suomalainen A, Vehmas T, Kortesniemi M, Robinson S, Peltola J. Accuracy of linear measurements using dental cone beam and conventional multislice computed tomography. Dentomaxillofac Radiol 2008;37:10-7.
4. Tyndall DA, Brooks SL. Selection criteria for dental implant site imaging: A position paper of the American academy of oral and maxillofacial radiology. Oral Surg Oral Med Oral Pathol Oral Radiol Endod 2000;9:630-7.
5. International Commission on Radiological Protection. Recommendations of the International Commission on Radiological Protection. United Kingdom: ICRP Publication 60. Ann ICRP; 1991. p. 21.
6. Ludlow JB, Davies-Ludlow LE, Brooks SL. Dosimetry of two extraoral direct digital imaging devices: New Tom cone beam CT and Orthophos Plus DS panoramic unit. Dentomaxillofac Radiol 2003;32:229-34.
7. International Commission on Radiological Protection Recommendations of the International Commission on Radiological Protection. United Kingdom: ICRP Publication 26. Ann ICRP; 1976. p. 1.
8. White SC, Pharoah MJ. Oral Radiology: Principles and Interpretation. 5th ed. Philadelphia: Mosby; 2004.
9. Shapurian T, Damoulis PD, Reiser GM, Griffin TJ, Rand WM. Quantitative evaluation of bone density using the Hounsfield index. Int J Oral Maxillofac Implants 2006;21:290-7.
10. Turkyilmaz I, Tözüm TF, Tumer C. Bone density assessments of oral implant sites using computerized tomography. J Oral Rehabil 2007;34:267-72.
11. de Oliveira RC, Leles CR, Normanha LM, Lindh C, Ribeiro-Rotta RF. Assessments of trabecular bone density at implant sites on CT images. Oral Surg Oral Med Oral Pathol Oral Radiol Endod 2008;105:231-8.
12. Rinkel J, Gerfault L, Estève F, Dinten JM. A new method for X-ray scatter correction: First assessment on a cone-beam CT experimental setup. Phys Med Biol 2007;52:4633-52.
13. Draenert FG, Coppenrath E, Herzog P, Muller S, Mueller-Lisse UG. Beam hardening artefacts occur in dental implant scans with the new Tom cone beam CT but not with the dental 4-row multidetector CT. Dentomaxillofac Radiol 2007;36:198-203.
14. Chan HL, Brooks SL, Fu JH, Yeh CY, Rudek I, Wang HL. Cross-sectional analysis of the mandibular lingual concavity using cone beam computed tomography. Clin Oral Impl Res 2011;22:201-6.
15. Chen LC, Lundgren T, Hallström H, Cherel F. Comparison of different methods of assessing alveolar ridge dimensions prior to dental implant placement. J Periodontol 2008;79:401-5.
16. Kalpidis CD, Setayesh RM. Hemorrhaging associated with endosseous implant placement in the anterior mandible: A review of the literature. J Periodontol 2004;75:631-45.

17. Givol N, Chaushu G, Halamish-Shani T, Taicher S. Emergency tracheostomy following life threatening hemorrhage in the floor of the mouth during immediate implant placement in the mandibular canine region. J Periodontol 2000;71:1893-5.
18. Chan HL, Leong DJ, Fu JH, Yeh CY, Tatarakis N, Wang HL. The significance of the lingual nerve during periodontal/implant surgery. J Periodontol 2010;81:372-7.
19. Greenstein G, Cavallaro J, Romanos G, Tarnow D. Clinical recommendations for avoiding and managing surgical complications associated with implant dentistry: A review. J Periodontol 2008;79:1317-29.
20. Greenstein G, Cavallaro J, Tarnow D. Practical application of anatomy for the dental implant surgeon. J Periodontol 2008;79:1833-46.
21. Sammartino G, Marenzi G, Citarella R, Ciccarelli R, Wang HL. Analysis of the occlusal stress transmitted to the inferior alveolar nerve by an osseointegrated threaded fixture. J Periodontol 2008;79:1735-44.
22. Chiapasco M, Abati S, Romeo E, Vogel G. Clinical outcome of autogenous bone blocks or guided bone regeneration with e-PTFE membranes for the reconstruction of narrow edentulous ridges. Clin Oral Implants Res 1999;10:278-88.
23. Watanabe H, Mohammad Abdul M, Kurabayashi T, Aoki H. Mandible size and morphology determined with CT on a premise of dental implant operation. Surg Radiol Anat 2010;32:343-9.
24. Corpas Ldos S, Jacobs R, Quirynen M, Huang Y, Naert I, Duyck J. Peri-implant bone tissue assessment by comparing the outcome of intra-oral radiograph and cone beam computed tomography analyses to the histological standard. Clin Oral Impl Res 2011;22:492-9.
25. Snauwaert K, Duyck J, van Steenberghe D, Quirynen M, Naert I. Time dependent failure rate and marginal bone loss of implant supported prostheses: A 15-year follow-up study. Clin Oral Investig 2000;4:13-20.
26. Pikner SS. Radiographic follow-up analysis of Branemark dental implants. Swed Dent J Suppl 2008;19:5-69.
27. Naitoh M, Yoshida K, Nakahara K, Gotoh K, Ariji E. Demonstration of accessory mental foramen using rotational panoramic radiography compared with cone-beam computed tomography. Clin Oral Impl Res 2011;22:1415-9.
28. Naitoh M, Hiraiwa Y, Aimiya H, Ariji E. Observation of bifid mandibular canal using conebeam computed tomography. Int J Oral Maxillofac Implants 2009;24:155-9.
29. Sancbis JM, Penarroba M, Soler F. Bifid mandibular canal. Int J Oral Maxillofac Surg 2003;61:422-4.
30. Mraiwa N, Jacobs R, van Steenberghe D, Quirynen M. Clinical assessment and surgical implications of anatomic challenges in the anterior mandible. Clin Implant Dent Relat Res 2003;5:219-25.
31. Bornstein MM, Balsiger R, Sendi P, von Arx T. Morphology of the nasopalatine canal and dental implant surgery: A radiographic analysis of 100 consecutive patients using limited cone-beam computed tomography. Clin Oral Impl Res 2011;22:295-301.
32. Pietrokovski J, Starinsky R, Arensburg B, Kaffe I. Morphologic characteristics of bony edentulous jaws. J Prosthodont 2007;16:141-7.
33. Sanz M, Cecchinato D, Ferrus J, Pjetursson EB, Lang NP, Lindhe J. A prospective, randomized- controlled clinical trial to evaluate bone preservation using implants with different geometry placed into extraction sockets in the maxilla. Clin Oral Impl Res 2010;21:13-21.
34. Janua'rio AL, Duarte WR, Barriviera M, Mesti JC, Araujo MG, Lindhe J. Dimension of the facial bone wall in the anterior maxilla: A cone-beam computed tomography study. Clin Oral Impl Res 2011;22:1168-71.

How to cite this article: Gupta J, Ali SP. Cone beam computed tomography in oral implants. Natl J Maxillofac Surg 2013;4:2-6.

Source of Support: Nil. **Conflict of Interest:** None declared.